Article

Inhibition of BMP signaling with LDN 193189 can influence bone marrow stromal cell fate but does not prevent hypertrophy during chondrogenesis

Rose Ann G. Franco,[1,2] Eamonn McKenna,[1,2] Pamela G. Robey,[3] Md. Shaffiulah Shajib,[1,2,4] Ross W. Crawford,[1] Michael R. Doran,[1,2,3,4,5,6,*] and Kathryn Futrega[1,2,3,6,*]

[1]Centre for Biomedical Technologies, School of Mechanical, Medical and Process Engineering, Faculty of Engineering, Queensland University of Technology (QUT), Brisbane, Australia
[2]Translational Research Institute, Brisbane, Australia
[3]Skeletal Biology Section, National Institute of Dental and Craniofacial Research, National Institutes of Health, Department of Health and Human Services, Bethesda, MD, USA
[4]School of Biomedical Sciences, Faculty of Health, Queensland University of Technology, Brisbane, Australia
[5]Mater Research Institute – University of Queensland, Brisbane, Australia
[6]Co-senior authors
*Correspondence: michael.doran@qut.edu.au (M.R.D.), futregak2@nih.gov (K.F.)
https://doi.org/10.1016/j.stemcr.2022.01.016

SUMMARY

Bone morphogenetic protein (BMP) cascades are upregulated during bone marrow-derived stromal cell (BMSC) chondrogenesis, contributing to hypertrophy and preventing effective BMSC-mediated cartilage repair. Previous work demonstrated that a proprietary BMP inhibitor prevented BMSC hypertrophy, yielding stable cartilage tissue. Because of the significant therapeutic potential of a molecule capable of hypertrophy blockade, we evaluated the capacity of a commercially available BMP type I receptor inhibitor with similar properties, LDN 193189, to prevent BMSC hypertrophy. Using 14-day microtissue chondrogenic induction cultures we found that LDN 193189 permitted BMSC chondrogenesis but did not prevent hypertrophy. LDN 193189 was sufficiently potent to counter mineralization and adipogenesis in response to exogenous BMP-2 in osteogenic induction cultures. LDN 193189 did not modify BMSC behavior in adipogenic induction cultures. Although LDN 193189 is effective in countering BMP signaling in a manner that influences BMSC fate, this blockade is insufficient to prevent hypertrophy.

INTRODUCTION

Bone marrow-derived stromal cells (BMSCs, also sometimes referred to to as "mesenchymal stem cells") were once heralded as "a panacea for cartilage repair" (Somoza et al., 2014). These cells are relatively easy to harvest, expand *in vitro*, and yield cartilage-like tissue following *in vitro* chondrogenic induction. However, chondrogenically induced BMSCs appear to be fated toward endochondral ossification, forming mineralized tissue when implanted *in vivo*, which is not suitable for cartilage defect repair (Somoza et al., 2014). The significance of hypertrophy as a clinical barrier to BMSC-mediated cartilage repair is exemplified by the fact that no BMSC product has received regulatory approval or is being commercialized for cartilage defect repair (Negoro et al., 2018).

Different strategies have been proposed to obstruct or prevent BMSC hypertrophy, which include targeting key signaling pathways during *in vitro* chondrogenic induction by modulation of WNT signaling (Narcisi et al., 2015; Yang et al., 2012), addition of parathyroid hormone-related peptide (PTHrP) (Kim et al., 2008; Lee and Im, 2012), inhibition of Erk1/2 signaling (Kim and Im, 2009) or inhibition of bone morphogenic protein signaling (BMP) (Occhetta et al., 2018). There is reason to believe that obstructing

BMP signaling could reduce or prevent BMSC hypertrophy. In previous work, our group demonstrated that exposure of BMSCs to a single day of transforming growth factor β1 (TGF-β1) was sufficient to upregulate *BMP2* gene expression (Futrega et al., 2021). *BMP2* expression and hypertrophic signaling persisted even when exogenous TGF-β1 was removed from the medium after the first day of induction culture (Futrega et al., 2021), suggesting that BMP signaling is part of the intrinsic programming that drives hypertrophic processes.

We evaluated the capacity of LDN 193189 to modulate BMSC hypertrophy during chondrogenic induction culture. LDN 193189, a dorsomorphin derivative, is a potent and selective activin receptor-like kinase 2 (ALK2) and ALK3 inhibitor, which exhibits greater specificity for BMP receptors than dorsomorphin, even at reduced concentrations (Yu et al., 2008). This compound efficiently blocks the activation of the Smad 1/5/8 pathway (Boergermann et al., 2010), which was the pathway targeted in previous studies reporting stable BMSC chondrogenesis when an inhibitor molecule was used during culture (Dexheimer et al., 2016; Hellingman et al., 2010; Occhetta et al., 2018).

Herein, we used a small-diameter microtissue model to study chondrogenic and hypertrophic differentiation in response to various concentrations of LDN 193189.
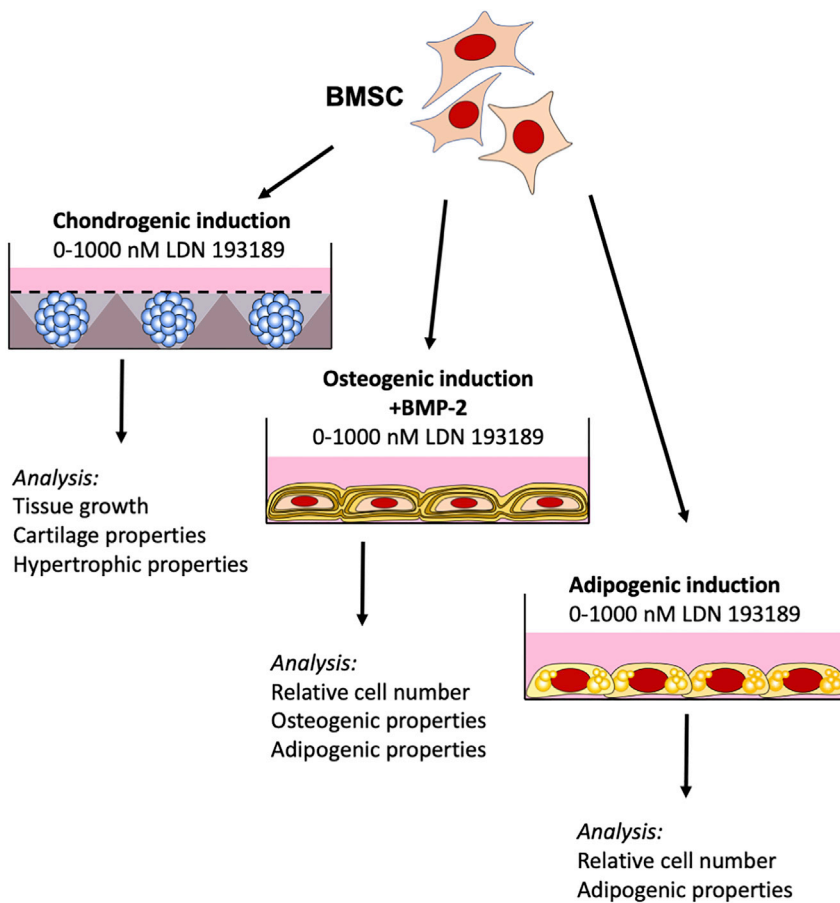
Figure 1. Schematic diagram of the experimental design
The schematic outlines the procedures used to assess the effect of BMP inhibitor LDN 193189 on BMSC microtissue chondrogenesis in the Microwell-mesh, monolayer osteogenesis, and monolayer adipogenesis.

Compared with larger-diameter traditional pellet cultures, smaller-diameter microtissues experience reduced diffusion gradients, yielding more homogeneous tissues that provide greater resolution for culture optimization (Babur et al., 2015; Futrega et al., 2015, 2021). We used a microwell platform, the Microwell-mesh (Futrega et al., 2015), to efficiently generate hundreds of uniformly sized BMSC microtissues. The Microwell-mesh is a culture platform that consists of a microwell array with a nylon mesh bonded over the microwell openings. The mesh pores are large enough to allow a single cell suspension to be centrifuged through the pores and pelleted at the bottom of the microwells. Once BMSCs self-assemble into microtissues, they are too large to escape back through the mesh and are retained in discrete microwells over the culture period. This method allows for the efficient manufacture of hundreds-to-thousands of microtissues and exchange of the medium without disturbing the microtissues. Because BMP signaling is also known to affect osteogenesis and adipogenesis (Futrega et al., 2018; Sottile and Seuwen, 2000), we evaluated the capacity of LDN 193189 to influence cell fate in osteogenic and adipogenic induction cultures.

RESULTS

The influence of BMP signaling inhibitor LDN 193189 on BMSC differentiation was evaluated in chondrogenic, osteogenic, and adipogenic cultures using the assays summarized schematically in Figure 1.

Effect of LDN 193189 on growth and GAG production in chondrogenic microtissues

When exposed to chondrogenic induction media for 1–2 weeks, BMSC microtissues increase in size and accumulate glycosaminoglycans (GAG) in the extracellular matrix (Futrega et al., 2015). Here, we evaluated microtissue growth and GAG production in the presence of LDN 193189. Microscopic examination of chondrogenic microtissue cultures revealed that increasing LDN 193189 concentrations had a negative effect on microtissue size (Figure 2A). Quantification of microtissue diameters on day 2, 8, and 14 for all four BMSC donors is shown in Figure 2B. Microtissue diameters were similar between conditions on day 2, but a pattern of reduced diameters was
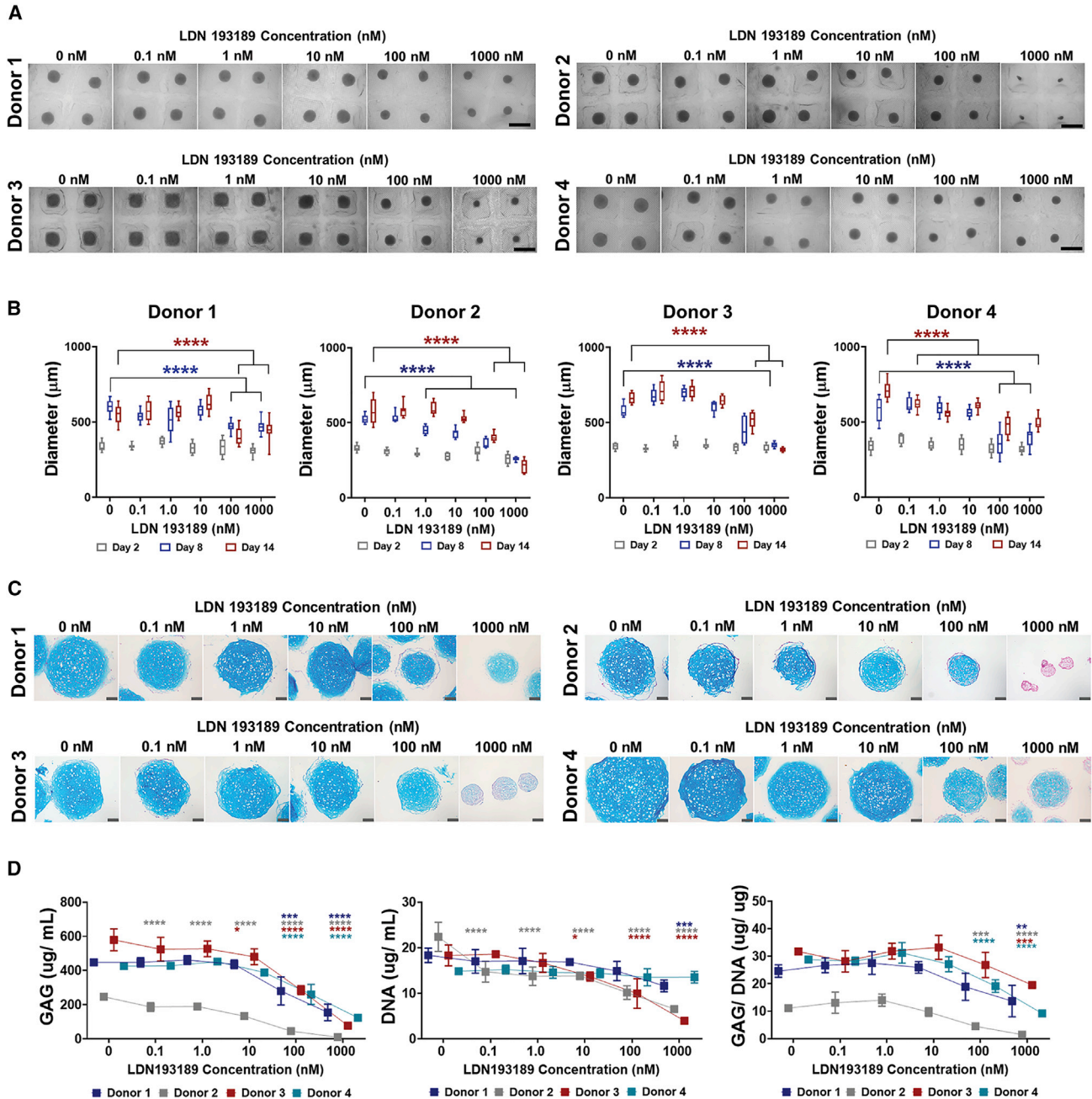
Figure 2. Growth of chondrogenic microtissues treated with various LDN 193189 concentrations

(A) Bright-field images of chondrogenic microtissues from Donors one to four1–4 on day 14 (scale bars, 1 mm).

(B) Average diameters of chondrogenic microtissues on days 2, 8, and 14. For boxplots, whiskers represent the minimum and maximum value, the center represents the median, and the edges of the box represent the first and third quartiles (n = 8 for each cell donor).

(C) Alcian blue-stained sections of day-14 microtissues (scale bars, 100 μm).

(D) GAG, DNA, and GAG/DNA quantification for microtissues cultured for 14 days. Connecting lines are added to aid in visualizing trends only.

Symbols represent means ± SD, n = 4 replicate cultures for each donor. *Statistically significantly different from the corresponding 0 nM control condition; *p < 0.05, **p < 0.01, ***p < 0.001, and ****p < 0.0001.
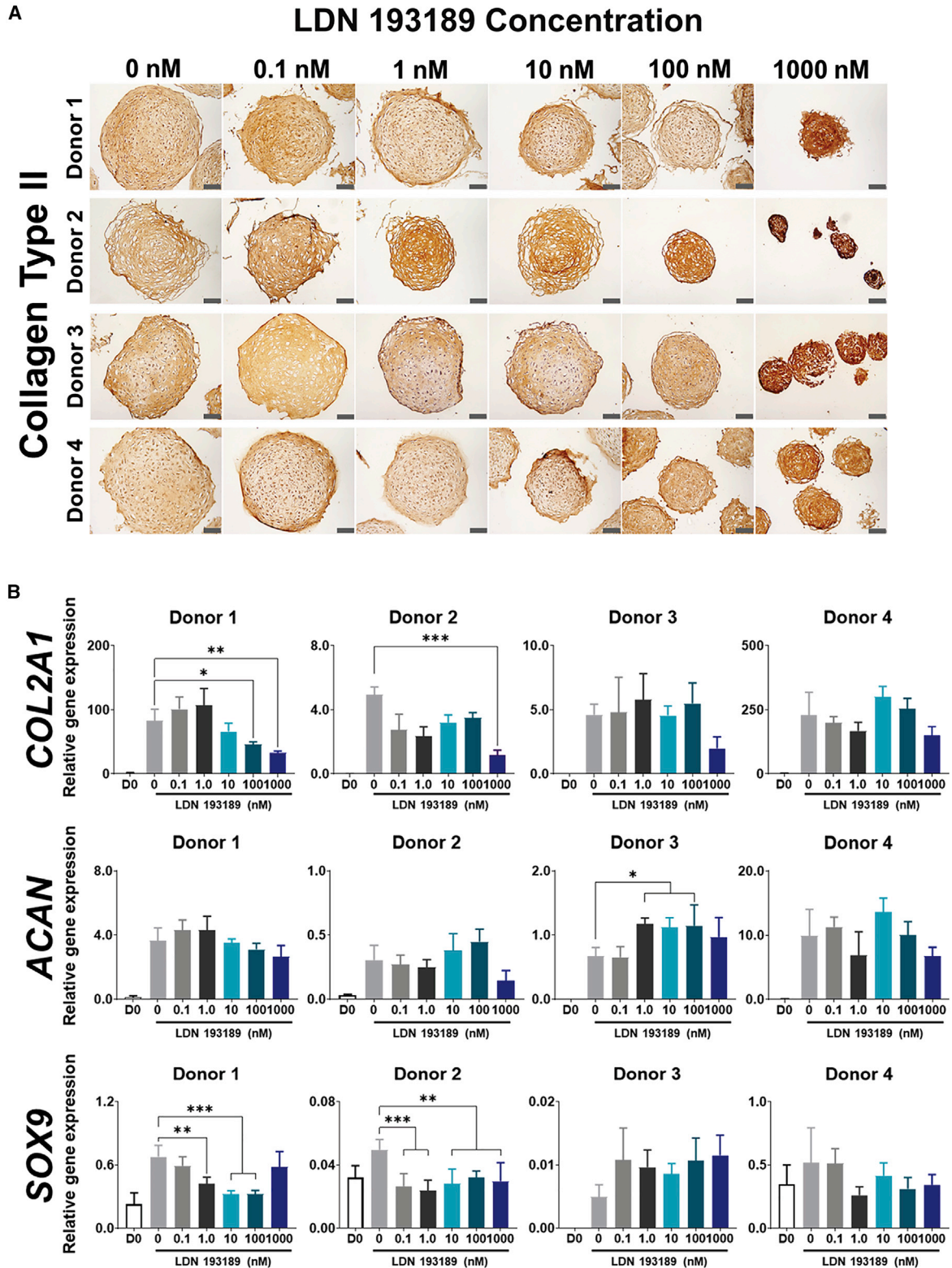
Figure 3. Effect of LDN 193189 on chondrogenic markers in microtissue cultures

(A) Immunohistological staining of collagen type II in microtissue sections from four BMSC donors treated with increasing concentrations of LDN 193189 for 14 days (scale bars, 100 μm). Controls for immunohistological staining are provided in Figure S1.

(legend continued on next page)

observed by day 8 with increasing LDN 193189 concentrations. By day 14, microtissues from all BMSC donors treated with ≥100 nM LDN 193189 had reduced diameters compared with vehicle control microtissues (Figure 2B).

To assess the deposition of GAG, we stained day-14 microtissue sections with Alcian blue. For LDN 193189 concentrations less than 1,000 nM, microtissues maintained intense GAG staining and exhibited lacunae structures characteristic of mature cartilage tissue; however, these features were diminished at 1,000 nM LDN 193189 (Figure 2C). For Donor 2 and Donor 3, a dense and compact fibrous tissue was observed without the intense blue stain indicative of GAG at 1,000 nM LDN 193189.

We further quantified GAG and DNA in microtissues by use of the dimethylmethylene blue assay (DMMB) and PicoGreen assay, respectively (Figure 2D). For LDN 193189 concentrations ≥100 nM, GAG quantity in microtissues decreased for all BMSC donors (Figure 2D). DNA content appeared to decline with increasing LDN 193189 concentrations, but this was statistically significant for only two donors at 100 nM and three donors at 1,000 nM (Figure 2D). When GAG was normalized to DNA, a statistically significant reduction in GAG/DNA was observed for two of four donors at 100 nM and for all four donors at 1,000 nM LDN 193189 (Figure 2D).

Effect of LDN 193189 on chondrogenic markers in microtissue cultures

We assessed the effect of LDN 193189 on markers associated with chondrogenesis by use of immunohistochemistry and gene expression analysis (Figure 3). The addition of LDN 193189 did not affect collagen type II staining at ≤ 100 nM LDN 193189 (Figure 3A). At 1,000 nM LDN 193189, darker collagen type II staining was observed; however, we believe that denser collagen networks may be attributable to reduced GAG matrix content (Figures 2C and 2D) rather than to greater collagen production in these microtissues.

The effect of LDN 193189 on the expression of gene markers associated with chondrogenesis (*COL2A1, ACAN,* and *SOX9*) was evaluated for all BMSC donors on day 14 (Figure 3B). *COL2A1* and *ACAN* are late markers of chondrogenesis, while *SOX9* is an early chondrogenic transcription factor (Amin et al., 2014). *COL2A1* expression appeared to be reduced at higher concentrations (100 and 1,000 nM) of LDN 193189, but this was statistically significant for only two of four BMSC donors tested. Expression of *ACAN* was not downregulated by LDN 193189 treatment

for all BMSC donors. A consistent effect of LDN 193189 on *SOX9* expression was not observed across all BMSC donors. Although there were some modest differences in the expression of chondrogenic marker genes in response to varying LDN 193189 concentrations, these differences were not always consistent across all BMSC donors, nor were they consistently statistically significant.

Effect of LDN 193189 on hypertrophic markers in microtissue cultures

We assessed the effect of LDN 193189 on markers associated with BMSC hypertrophy by use of immunohistochemistry and gene expression analysis (Figure 4). Collagen type X immunohistochemical staining did not appear to be affected when the medium was supplemented with LDN 193189, with positive staining visible in all microtissues from all BMSC donors (Figure 4A). Intense collagen type X staining was observed in microtissue sections treated with 1,000 nM LDN 193189, but, as with collagen type II staining, this was attributed to a denser collagen network resulting from reduced matrix GAG content rather than to an increase in collagen type X in these tissues.

Several markers are associated with chondrogenic hypertrophy or osteogenic mineralization, including *COL10A1, RUNX3, MEF2C* (Dreher et al., 2020), *VEGF* (Wu et al., 2021), *COL1A1,* and *SP7* (Kovermann et al., 2019). Exposure to LDN 193189, even at the highest concentrations, did not suppress the expression of these hypertrophic genes in a manner that was consistent across all four BMSC donors (Figure 4B). *COL10A1* was significantly reduced when Donor 2 microtissues were exposed to ≥100 nM LDN 193189. However, this may not have been a specific downregulation of hypertrophic processes, as there was a corresponding decrease in chondrogenic gene expression (*COL2A1* and *SOX9*; Figure 3B). Exposure to 1,000 nM LDN 193189 elevated *RUNX3* for Donor 3, elevated *MEF2C* for Donors 1, 3, and 4, and elevated *SP7* for Donors 1, 3, and 4. No reduction in pro-hypertrophic properties was observed on the basis of the *COL10A1/COL2A1* ratio in any of the BMSC donors (Figure 4C). An increase in *COL10A1/COL2A1* was observed in Donor 1 and Donor 4 microtissues when exposed to 1,000 nM.

Effect of LDN 193189 on osteogenic induction cultures

BMP-2 is known to induce BMSC osteogenesis (Futrega et al., 2018). To assess the capacity of LDN 193189 to inhibit BMP-2 signaling, we evaluated whether LDN

(B) Gene expression analysis of chondrogenic markers (*COL2A1, ACAN,* and *SOX9*) in microtissues cultured for 14 days.
Bar graphs represent means ± SD, n = 4 replicate cultures for each donor. *Significantly different from the corresponding 0 nM control; *p < 0.05, **p < 0.01, ***p < 0.001, and ****p < 0.0001.
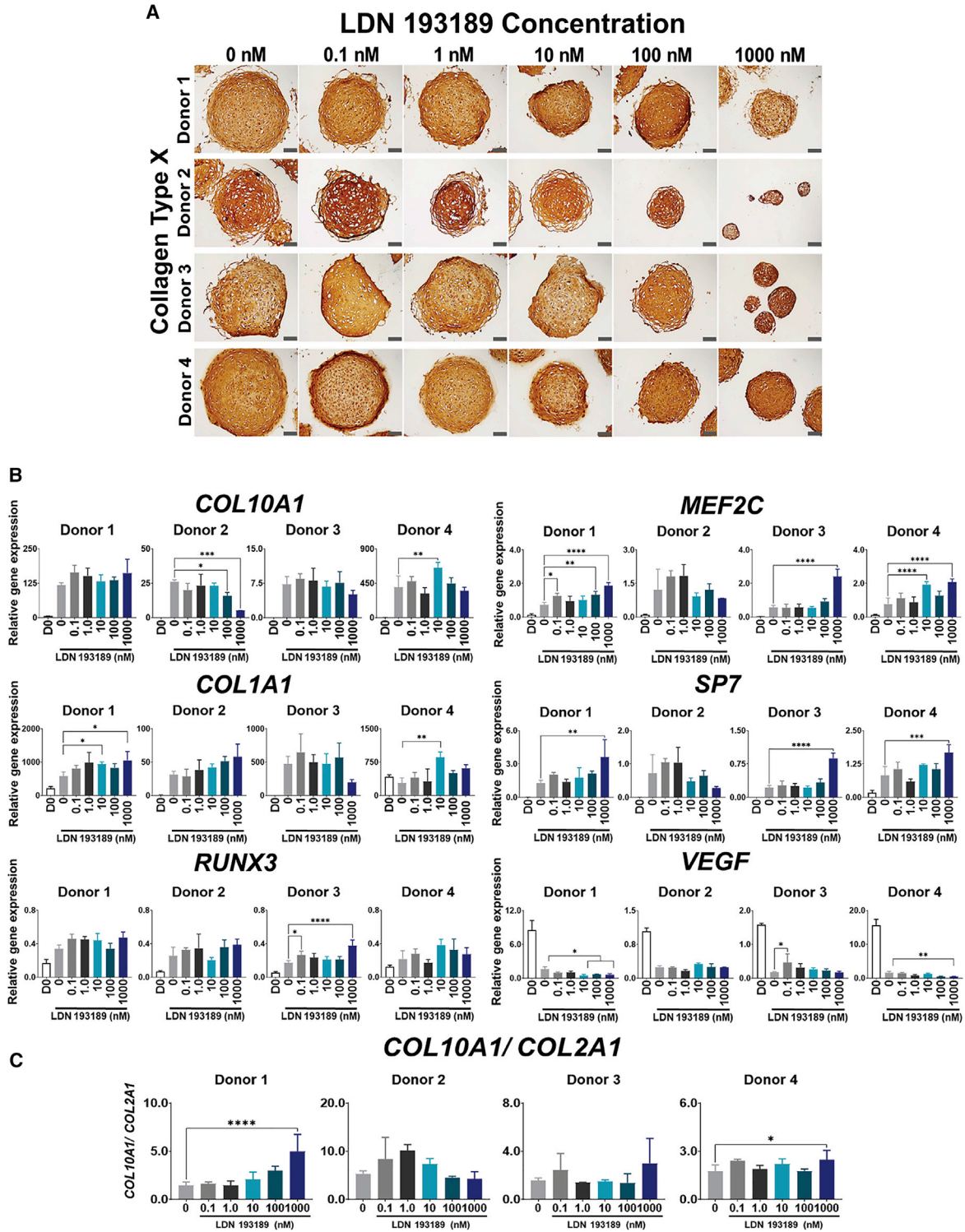
Figure 4. Effect of LDN 193189 on hypertrophic markers in chondrogenic cultures

(A) Immunohistological staining of collagen type X in microtissue sections from all BMSC donors on day 14 of chondrogenic culture (scale bars, 100 μm). Controls for immunohistological staining are provided in Figure S1.

(legend continued on next page)

193189 countered the effect of exogenous BMP-2 in BMSC osteogenic monolayer cultures. The concentration of BMP-2 supplementation in osteogenic medium was first optimized by performing a titration assay using increasing concentrations of BMP-2 (0, 1, 10, 50, 100, and 500 ng/mL) and four BMSC donors. After 14 days of culture, significant mineralization was observed for BMP-2 concentrations of ≥50 ng/mL as detected by alizarin red S staining (Figures S2A and S2B). We also attempted to measure relative cell viability using the alamarBlue assay; however, spontaneous delamination occurred by this 14-day time point in some wells, irrespective of mineralization, and compromised the fidelity of such assessment (Figure S2C). In subsequent osteogenic assays, where indicated, we used 100 ng/mL BMP-2 and with shorter culture times (9 days) to avoid monolayer delamination.

Using the alamarBlue assay as a measure of relative cell number or viability, we found that the addition of LDN 193189 from 0.1 to 1,000 nM did not significantly compromise cell viability relative to 0 nM controls (Figure 5A, black squares). These data suggest that the addition of LDN 193189 did not have a cytotoxic effect on cells following 9 day of osteogenic induction culture.

Osteogenic induction cultures were characterized for calcium deposition by use of the spectrophotometric o-Cresolphthalein complexone (OCPC; Figure 5A) assay and alizarin red S staining (Figures 5A, 5B, and S3A). Relative to control osteogenic cultures, the addition of BMP-2 significantly increased the amount of calcium deposition after 9 days of induction for BMSC Donors 1, 3, and 4 (Figure 5A). The OCPC assay revealed a reduction in calcium accumulation in monolayers starting at an LDN 193189 concentration of 0.1 nM for Donor 3, 10 nM for Donor 4 and 100 nM for Donor 1. Alizarin red S staining mimicked the results of the OCPC assay, with negligible staining of the well surface at ≥100 nM LDN 193189 for Donors 1, 3, and 4 (Figure 5B). Mineralization was not observed in Donor 2 monolayers after 9 days (Figures 5A and 5B); however, when the induction time was extended to 18 days, the effect of BMP-2 addition and BMP-2 inhibition by LDN 193189 (starting at 100 nM) was evident using alizarin red S staining, and comparable to the other three donors (Figure S3B).

We performed gene expression analysis of osteogenic markers (RUNX2, ALPL, and SP7) for the following conditions: day 0 (D0) cells from expansion cultures, non-induced (NI) vehicle control, 0 nM LDN 193189 + BMP-2, and 100 nM LDN 193189 + BMP-2. Osteogenic gene

markers RUNX2, ALPL, and SP7 were elevated in BMP-2 supplemented medium relative to osteogenic medium that did not include BMP-2 across all donors (Figures 5C and S3B). Except for Donor 1, the increase in ALPL driven by BMP-2 was abrogated by the addition of LDN 193189 to the medium. The addition of LDN 193189 to cultures containing BMP-2 annulled SP7 gene expression for all BMSC donors.

Effect of LDN 193189 on adipogenesis in osteogenic cultures

Previous studies demonstrated that BMP-2 medium supplementation not only induces osteogenesis but also induces BMSC adipogenesis (Futrega et al., 2018; Sottile and Seuwen, 2000). Here, we quantified the prevalence of lipid vacuoles in BMSC osteogenic cultures supplemented with BMP-2 and LDN 193189. First, we confirmed that the addition of BMP-2 to osteogenic induction medium resulted in widespread formation of lipid vacuoles in all BMSC donors, as accentuated by oil red O staining (Figure 6A). A significant reduction in oil red O-positive lipid vacuoles was observed when cultures were supplemented with ≥100 nM LDN 193189 (Figure 6A). A gradual reduction in lipid vacuoles was seen with increasing LDN 193189 concentrations across all BMSC donors (Figure 6B, red squares). When plotted with the OCPC data, lipogenesis paralleled calcium accumulation, except for Donor 2, where mineralization was delayed (Figures 5B and S3B). Adipogenic gene markers PPARG and FABP4 increased significantly in osteogenic cultures supplemented with BMP-2, relative to induction cultures lacking BMP-2 (Figure 6C). The addition of 100 nM LDN 193189 significantly reduced the expression of both adipogenic genes and appeared to be sufficient to block extrinsic BMP-2-mediated adipogenesis in BMSC osteogenic cultures (Figure 6C).

Effect of LDN 193189 on adipogenic cultures

Last, we tested whether LDN 193189 influenced 21-day BMSC adipogenic induction cultures. The alamarBlue assay revealed essentially no metabolic differences between adipogenic cultures treated with 0.1–100 nM LDN 193189 compared with non-treated controls (0 nM), for all BMSC donors (Figure 7A). However, the highest LDN 193189 concentration of 1,000 nM resulted in a sharp drop in cell viability (Figure 7A, black squares) and reduced cell number was confirmed microscopically (Figure 7B). Oil red O staining revealed that substantial lipid vacuoles were formed up to the 100 nM LDN 193189 treatment for all donors, after which

(B) Relative gene expression of hypertrophic markers (COL1A1, COL10A1, MEF2C, RUNX3, SP7, and VEGF) in microtissues on day 14.
(C) Exposure to LDN 193189 did not reduce the COL10A1/COL2A1 ratio in any BMSC donors, relative to 0 nM controls on day 14.
Bar graphs represent means ± SD, n = 4 replicate cultures for each donor. *Statistically significantly different from the corresponding 0 nM control; *p < 0.05, **p < 0.01, ***p < 0.001, and ****p < 0.0001.
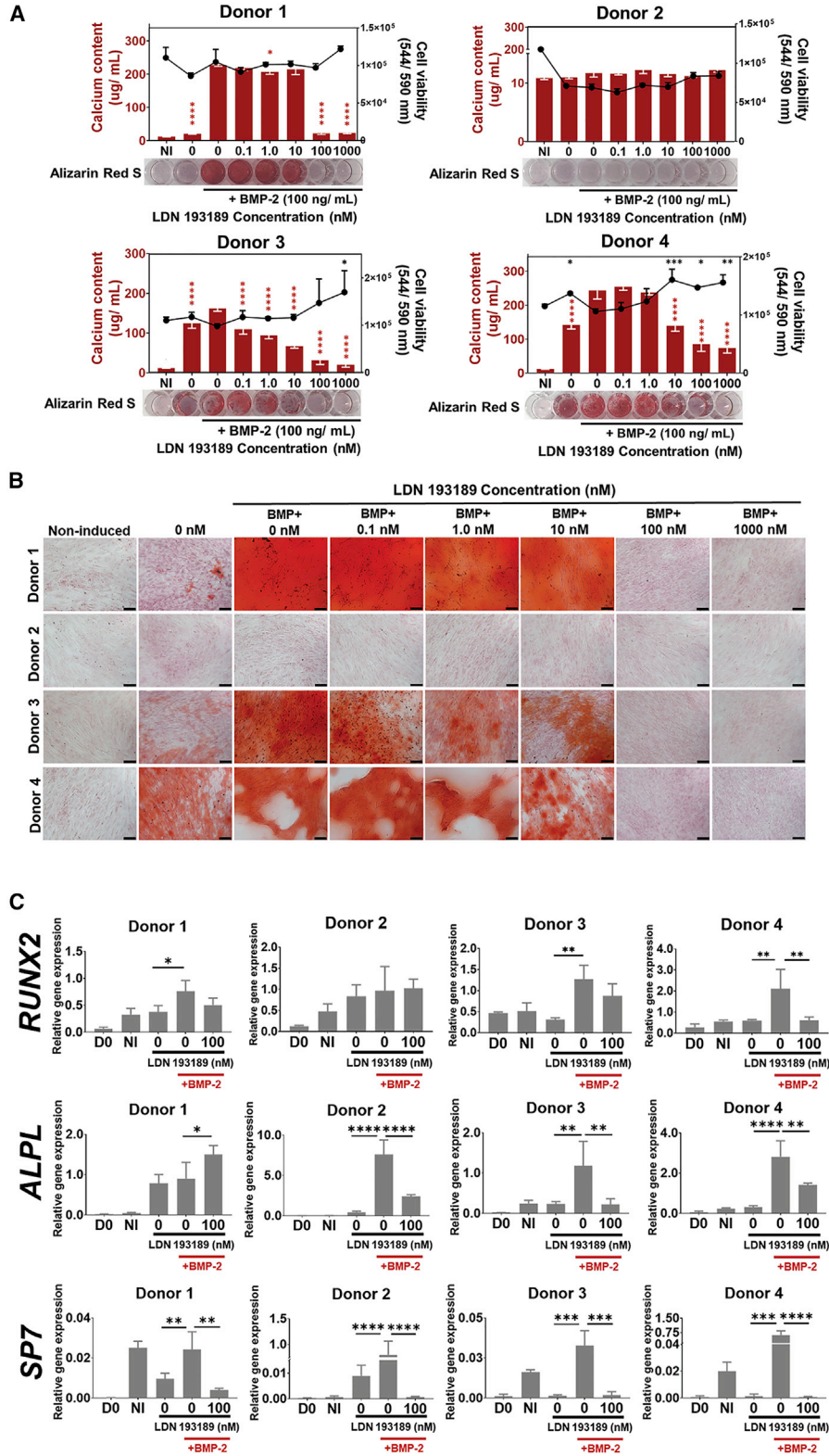
(legend on next page)

cell viability was compromised (Figures 7A and 7B). Image analysis was used to quantify lipid vacuoles, revealing significant donor variability. Whereas Donors 1 and 2 did not show a difference in lipid vacuole accumulation with increasing LDN 193189 concentrations, Donors 3 and 4 appeared to show a reduction in lipid vacuole area (Figure 7A, bar graphs). Expression of adipogenic gene markers (*PPARG* and *FABP4)* was assessed using cultures treated with 10–100 nM of the inhibitor, as this concentration reduced lipogenesis in two of four donors and did not appear to be cytotoxic. *PPARG* and *FABP4* were not consistently affected by the addition of LDN 193189 in adipogenic cultures across all four donors (Figure 7C).

DISCUSSION

For BMSCs to be useful in cartilage defect repair they must be guided to form stable chondrocyte-like cells and maintain this stable phenotype *in vivo*. Current BMSC chondrogenic induction media, most of which contain one of the TGF-β isoforms (TGF-β1, -β2 or -β3) (Freyria and Mallein-Gerin, 2012; Goldberg et al., 2017; Handorf and Li, 2014; Jakobsen et al., 2014; Puetzer et al., 2010), appears to engage intrinsic differentiation programming reminiscent of endochondral ossification (Futrega et al., 2021; Somoza et al., 2014). In a recent study, we demonstrated that as little as a single day of TGF-β1 exposure was sufficient to trigger BMP-2 signaling and hypertrophic gene cascades in BMSC chondrogenic cultures that persisted even if TGF-β1 was subsequently withdrawn from the medium (Futrega et al., 2021). These data suggested that BMP-2 signaling could be driving or maintaining hypertrophic processes and that targeting the BMP pathway might inhibit hypertrophy.

Previous studies have shown that TGF-β and BMP rely on Smad 2/3 and Smad 1/5/8 phosphorylation, respectively (Dexheimer et al., 2016). Blocking Smad 2/3 phosphorylation using the inhibitor SB-505124 prevented chondrogenic differentiation, whereas inhibition of Smad 1/5/8 phosphorylation by 10 μM dorsomorphin prevented terminal differentiation and mineralization (Hellingman et al., 2010). Dorsomorphin targets ALK1, ALK2, ALK3, and ALK6 receptors, and, when added at high concentra-

tions (10 μM) at the start of induction cultures, it down regulates *SOX9* gene expression in either BMP-4/7 or TGF-β1 supplemented cultures, preventing chondrogenesis (Dexheimer et al., 2016). ALK1 is essential for BMSC chondrogenesis (Marcu et al., 2015); thus, it is logical to assume that early addition of dorsomorphin might impair chondrogenesis. For an inhibitor like dorsomorphin, which targets ALK1, to be effective, BMSC chondrogenesis and hypertrophy would likely have to be sequential events whereby a chondrogenic program precedes a separate and targetable hypertrophic program. However, in recent studies we observed that both chondrogenic and hypertrophic programs are upregulated in BMSCs following the first day of TGF-β1 exposure (Futrega et al., 2021), and we reasoned that hypertrophy modulation is required from the start of chondrogenic induction. These data also suggest that chondrogenic and hypertrophic differentiation programs may be intertwined, potentially making it challenging to dampen one process and not affect the other.

Recently, Occhetta and colleagues demonstrated that a proprietary BMP signal inhibitor (Compound A), which selectively inhibited ALK2 and ALK3, enabled the generation of stable cartilage from BMSCs (Occhetta et al., 2018). Their cells did not express hypertrophy markers or form mineralized tissue when implanted *in vivo*. Like the compound described by Occhetta and colleagues, the commercially available molecule LDN 193189 is a selective and potent inhibitor of ALK2 and ALK3 receptor signaling (Yu et al., 2008). LDN 193189 blocks Smad 1/5/8 phosphorylation, similar to dorsomorphin, without the "off-target" effects (Boergermann et al., 2010), and it is effective at lower concentrations than dorsomorphin (Yu et al., 2008). A more recent publication from Occhetta and colleagues provides evidence that LDN 193189 also blocks ALK6, but they focus on how ALK2 and ALK3 inhibition using either Compound A or LDN 193189 dampened the hypertrophic phenotype of chondrocytes harvested from osteoarthritic joints (Chawla et al., 2020). These reports suggest that LDN 193189 may be a viable tool to prevent BMSC hypertrophy, and here we assessed its capacity to do so in chondrogenic induction cultures by using four unique BMSC donors.

We titrated LDN 193189 in chondrogenic cultures with the goal of identifying a non-toxic concentration that

Figure 5. The effect of LDN 193189 on osteogenic induction cultures
(A) Quantification of calcium accumulation in osteogenic cultures using OCPC assay, alamarBlue assay quantifying cell viability, and alizarin red-stained wells for mineralization.
(B) Microscopic images of monolayers stained with alizarin red S after 9 days of osteogenic induction (scale bars, 100 μm). Mineralization was delayed for Donor 2, but when cultures were extended, the assay yielded results similar to Donors 1, 3, and 4 (See Figure S3B).
(C) Relative gene expression of osteogenesis markers in osteogenic induction cultures. Day 0 (D0) corresponds to non-induced cells at time of cell seeding. Non-induced (NI) cells were cultured in basal media that contained no induction factors.
Data represent means ± SD, n = 3 replicate cultures for each donor. *Statistically significantly different from the corresponding 0 nM LDN 193189 + BMP-2 condition; *p < 0.05, **p < 0.01, ***p < 0.001, and ****p < 0.0001.
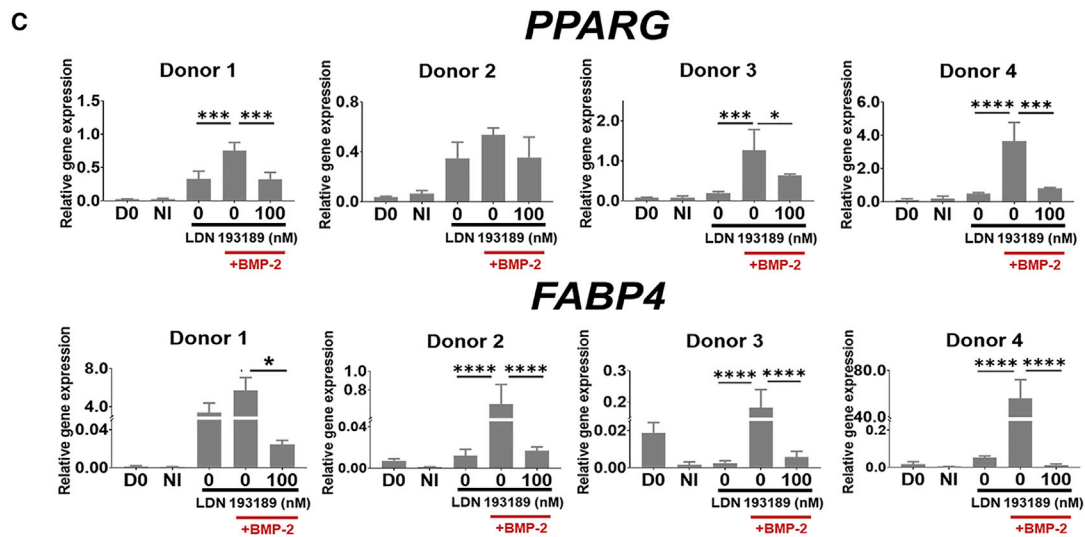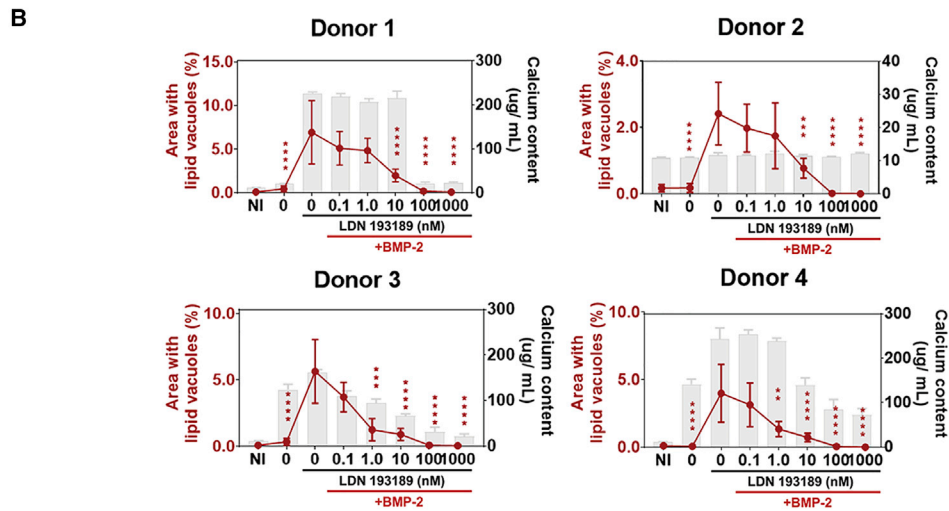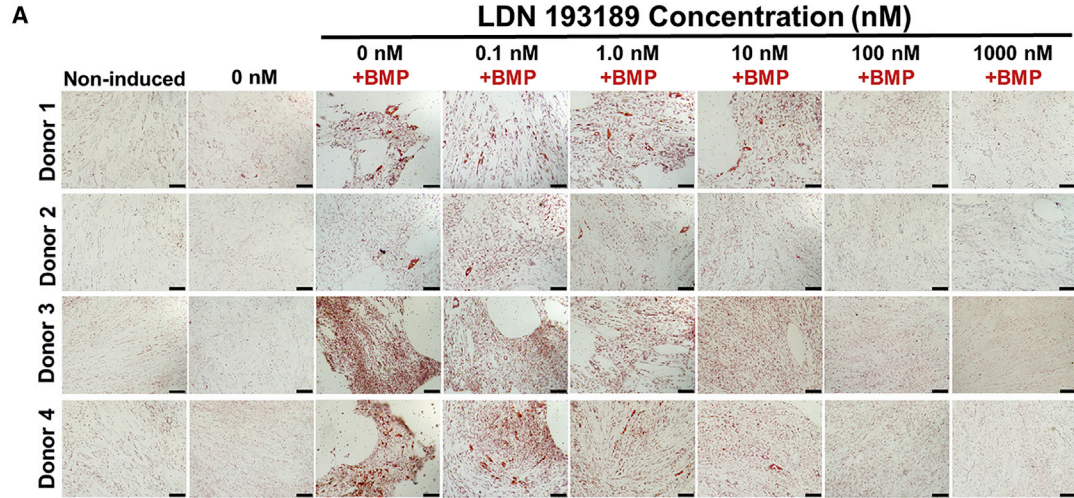
(legend on next page)

would permit chondrogenesis but obstruct hypertrophy. The addition of 0.1–10 nM LDN 193189 generally did not affect the growth of chondrogenically induced BMSC microtissues. At LDN 193189 concentrations of 100 nM, microtissue diameter and GAG matrix content were significantly reduced, but DNA content was minimally affected for two of four donors. Increasing the LDN 193189 concentration to 1,000 nM appeared to be cytotoxic, resulting in a significant reduction in microtissue diameter, reduction of lacunae, reduced GAG content in the extracellular matrix, and reduced DNA content for three of four donors. A previous study demonstrated that obstructing proliferation can obstruct BMSC chondrogenesis (Dexheimer et al., 2012), whereas another study associated BMSC proliferation capacity with successful chondrogenesis (Cleary et al., 2017). Inhibition of proliferation is a possible mechanism by which the highest concentration (1,000 nM) of LDN 193189 might inhibit chondrogenesis.

Some dampening of chondrogenesis would be tolerable if hypertrophy was effectively obstructed. While 100 nM LDN 193189 did have a modest negative impact on chondrogenesis, the microtissues continued to exhibit lacunae structures and ECM reminiscent of cartilage-like tissue. However, hypertrophic markers (*COL10A1*, *MEF2C*, *COL1A1*, *SP7*, *RUNX3*, and *VEGF*) were not significantly modified in a reproducible manner across all donors. This suggests that although chondrogenesis was still viable at up to 100 nM LDN 193189, hypertrophy was not obstructed.

The inability of LDN 193189 to obstruct hypertrophy in chondrogenic microtissues prompted us to assess the capacity of LDN 193189 to modulate BMP signaling in BMSCs by use of osteogenesis and adipogenesis assays. BMP-2 is a potent inducer of BMSC osteogenesis (Futrega et al., 2018) and was observed, here, to increase the expression of osteogenic gene markers and induce mineralization in 9-day monolayer cultures. The addition of LDN 193189 at ≥100 nM countered the effect of exogenously added BMP-2 (100 ng/mL), as evidenced by reduced alizarin red S staining and reduced expression of osteogenic genes (*RUNX2*, *ALPL*, and *SP7*). We did not observe toxicity in response to any LDN 193189 concentration in osteogenic cultures based on the alamarBlue assay, indicating that the inhibitor was functioning by countering BMP signaling rather than having a toxic effect.

BMP signaling is also known to play a role in adipogenic differentiation (Katagiri and Watabe, 2016; Takada et al., 2012), and our own previous studies have reported increased lipid vacuole formation in BMSC osteogenic cultures supplemented with BMP-2 (Futrega et al., 2018). To further assess the capacity of LDN 193189 to counter BMP signaling, we quantified adipogenesis in BMP-2-supplemented osteogenic cultures. Here, we found, in BMSC osteogenic cultures, an increase in lipid vacuole formation and upregulation of adipogenic gene markers (*PPARG* and *FABP4*) with the addition of exogenous BMP-2 to the culture medium. In response to BMP-2 stimulation, lipid vacuole formation even preceded mineralization in Donor 2 cultures (Figures 6B and S3B). A previous study had found that BMP-2 induced adipogenesis in C_2C_{12} cells, a myoblast cell line, and that adipogenesis was inhibited by the addition LDN 193189 via targeting of Smad 1/5/8 signaling (Boergermann et al., 2010). Similarly, we observed that increasing concentrations of LDN 193189 countered the effect of BMP-2-induced adipogenesis in osteogenic cultures, with the complete absence of visible lipid vacuoles at ≥100 nM of LDN 193189.

Finally, we sought to determine whether LDN 193189 influenced BMSC adipogenic induction cultures. These cultures used standard adipogenic induction medium and were not supplemented with exogenous BMP-2. In BMSC adipogenic differentiation cultures, lipid vacuole formation was evident up to 100 nM treatment of LDN 193189. LDN 193189 supplementation did not significantly affect the expression of *PPARG*, the master regulator of adipogenesis (Rosen et al., 2002) except in Donor 3 cultures. Reduced *FABP4* expression in response to LDN 193189 supplementation was only observed in Donor 4 cultures. Increasing the LDN 193189 concentration to 1,000 nM halted lipogenesis, but alamarBlue data suggested that this was likely due to toxicity rather than the specific abrogation of BMP signaling. Thus, although LDN 193189 blocked BMP-induced adipogenesis in osteogenic cultures, it did not appear to obstruct the non-BMP-mediated pathways that drive BMSC adipogenesis in standard adipogenic induction medium.

Our overall aim was to target BMP signaling with LDN 193189 and prevent BMSC hypertrophy. Whereas LDN 193189 abolished the effect of exogenous BMP-2 in osteogenic cultures, it did not prevent hypertrophy in BMSC

Figure 6. Effect of LDN 193189 on adipogenesis in osteogenic cultures
(A) Oil red 0-stained lipid vacuoles following 9 days of osteogenic differentiation (scale bars, 100 μm).
(B) Lipid vacuole and calcium quantification in osteogenic cultures treated with LDN 193189.
(C) Gene expression of adipogenic markers in osteogenic cultures. Day 0 (D0) corresponds to non-induced cells at time of cell seeding. Non-induced (NI) cells were cultured in basal media containing no induction factors.
Data represent means ± SD, n = 3 replicate cultures for each donor. *Statistically significantly different from the corresponding 0 nM LDN 193189 + BMP-2 condition; *p < 0.05, **p < 0.01, ***p < 0.001, and ****p < 0.0001.
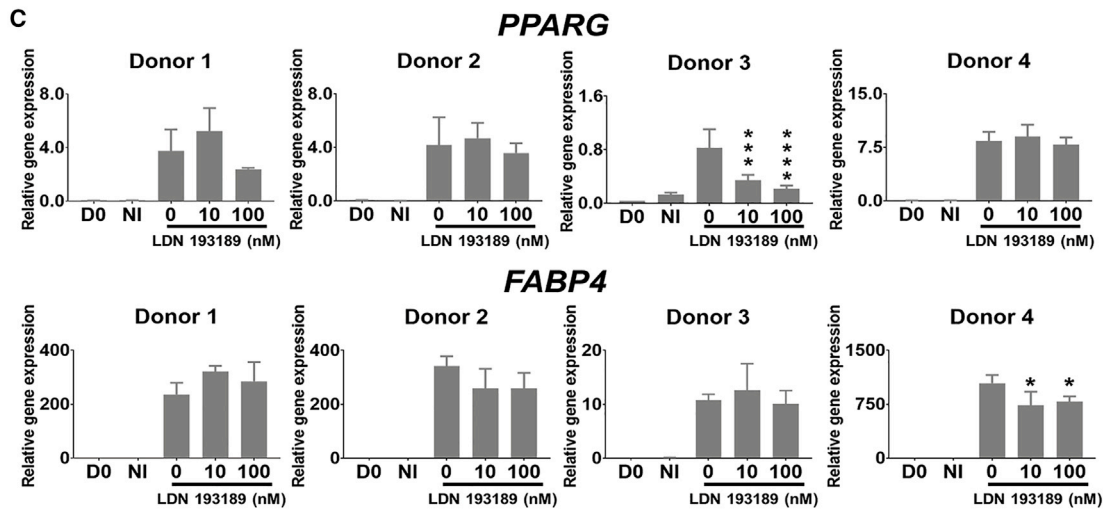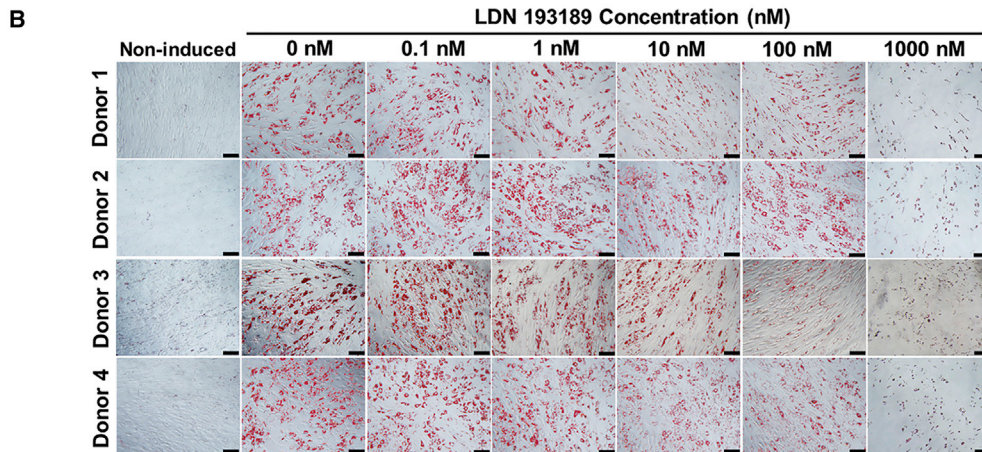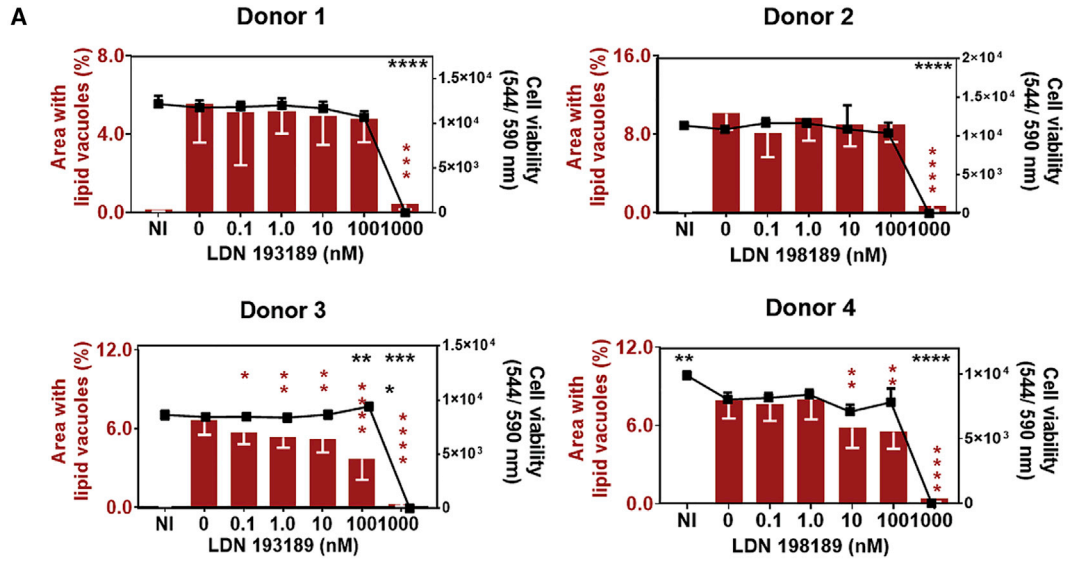
chondrogenic cultures. A major difference between our study and historical studies, was our use of a small-diameter microtissue cartilage model. Here, microtissues were assembled from 5×10^3 BMSCs each. By contrast, most historical studies used macrotissue models. For example, Occhetta and colleagues assembled tissues from 2.5×10^5 BMSCs each (Occhetta et al., 2018), whereas Dexheimer and colleagues assembled tissues from 5×10^5 BMSCs each (Dexheimer et al., 2016). A challenge with large-diameter macrotissues is that steep diffusion gradients form through the tissues, resulting in radially heterogeneous cell behavior (Futrega et al., 2021; Markway et al., 2010). By contrast, small-diameter microtissues suffer reduced gradients, and cells in these tissues behave more uniformly. Using a microtissue model, we previously demonstrated that a single day of TGF-β1 exposure was sufficient to induce chondrogenesis throughout the microtissue (Futrega et al., 2021). By comparison, differentiation appeared to progress incrementally from the surface to the interior of macrotissues over 2–3 weeks of TGF-β1 exposure. Because of this radial heterogeneity, histology slices taken from different regions of the same macrotissue may be significantly different. Consequently, if an inhibitor influences a specific stage of differentiation (i.e., early or late), some portions of the macrotissue may be affected differently than others, potentially confounding analysis. A possible benefit of a macrotissue model is that the delay in differentiation (Futrega et al., 2021) might provide more time for an inhibitor to function and delay or obstruct hypertrophy.

A logical next step in the search for molecules that prevent hypertrophy would be to perform a direct comparison of LDN 193189 with the proprietary BMP inhibitor Compound A (Occhetta et al., 2018) in BMSC chondrogenic assays, using both micro- and macrotissue models. While Occhetta and colleagues' recent publication suggests that LDN 193189 and Compound A have similar influence on chondrocytes harvested from osteoarthritic joints (Chawla et al., 2020), chondrocytes behave differently from BMSCs (Futrega et al., 2021), and this comparison needs to be performed on BMSCs. It is possible that the mode of action of Compound A on BMSC differentiation is slightly different than anticipated, and different from LDN 193189. Such data would add value to the literature, perhaps identifying other targets in the intrinsic programming that require

modulation for the generation of stable and non-hypertrophic BMSC-derived cartilage tissue.

EXPERIMENTAL PROCEDURES

BMSC isolation and expansion

Four BMSC donor cell populations were used in this study: Donor 1 was a 43-year-old male, Donor 2 was a 24-year-old male, Donor 3 was a 44-year-old male, and Donor 4 was a 21-year-old female. BMSCs were isolated as described previously (Futrega et al., 2015, 2021). In brief, bone marrow aspirates were collected from consenting voluntary donors by use of protocols approved by the Mater Hospital Human Research Ethics Committee and in accordance with National Health and Medical Research Council of Australia guidelines (Ethics number: 1541A). Using Ficoll-Paque PLUS density gradient (GE Healthcare) centrifugation, mononuclear cells were enriched from 20 mL of bone marrow aspirate. The mononuclear cells were resuspended in low-glucose Dulbecco's modified Eagle medium (LG-DMEM), supplemented with 10% fetal bovine serum (FBS, Thermo Fisher), 1% penicillin-streptomycin (PenStrep, Gibco), 10 ng/mL fibroblast growth factor 1 (FGF-1, PeproTech), and 5 μg/mL heparin (Sigma-Aldrich) (Futrega et al., 2015, 2021). The cells were distributed into five T175 flasks (Nunc) with 35 mL of growth medium in each flask, and placed into a humidified, normoxic incubator (20% O_2, 5% CO_2, and 37°C). On the following day, the medium was exchanged to enrich for adherent cells, and the cells were cultured in a hypoxic incubator (2% O_2, 5% CO_2, and 37°C) for further expansion. Hypoxic conditions were used for expansion to enhance BMSC proliferation (Grayson et al., 2006, 2007; Moussavi-Harami et al., 2004) and to maintain differentiation potential (Martin-Rendon et al., 2007; Zscharnack et al., 2009). Media exchange was performed every 3–4 days until 80% confluence. Cells were passaged at 2×10^5 cells per new T175 flask. BMSCs were used up to passage three in experiments.

Microwell-mesh fabrication

The Microwell-mesh is a high-throughput organoid or microtissue culture platform (Futrega et al., 2015). A diagram of the Microwell-mesh is provided in Figure 1. In brief, a polystyrene mold was used to cast an array of microwells in polydimethylsiloxane (PDMS, Sylgard184; Dow Corning). Discs were punched out of PDMS microwell array sheets with a wad punch and a nylon mesh (nylon 6-6, 36-μm-square openings) bonded over the microwell openings with a thin layer of silicon glue (Selleys Aquarium Safe). Discs with mesh attached were anchored into the bottom of six-well plates (Nunc) with a dab of silicone glue. Prior to use, wells were filled with 70% w/v ethanol, centrifuged

Figure 7. Adipogenic differentiation of BMSCs with LDN 193189 treatment after 21 days
(A) Lipid vacuole area and cell viability in adipogenic cultures treated with LDN 193189.
(B) Oil red O staining of lipid vacuoles in cell cytoplasms (scale bars, 100 μm).
(C) Gene expression of adipogenic markers in adipogenic cultures. Day 0 (D0) corresponds to non-induced cells at time of cell seeding. Non-induced (NI) cells were cultured in basal media that contained no induction factors.
Data represent means ± SD, n = 3 replicate cultures for each donor. *Statistically significantly different from the corresponding 0 nM LDN 193189 condition; *$p < 0.05$, **$p < 0.01$, ***$p < 0.001$, and ****$p < 0.0001$.

briefly at 1,000 × g to displace bubbles from microwells, and then entire plates soaked in ethanol for 1 h. Wells were rinsed three times with sterile water, dried at 60°C overnight, and stored until use. To make the microwell surface non-cell adherent, microwells were soaked for 5 min in a 5% pluronic F127 (Sigma-Aldrich) solution and then washed twice with PBS. The Microwell-mesh was used for 3D culture of BMSC-derived microtissues in the chondrogenic studies.

BMSC microtissue chondrogenic induction cultures

Cells were harvested from expansion cultures and seeded into six-well Microwell-mesh plates at a seeding density of 1.25×10^6 BMSC/well (~5,000 BMSC/microwell) in chondrogenic induction medium. To force cells into the microwells and promote cell aggregation, plates were centrifuged at 400 × g for 3 min. Chondrogenic induction medium contained high-glucose (HG)-DMEM supplemented with 1% PenStrep, 1% sodium pyruvate, 1% insulin-transferrin-selenium-ethanolamine solution (ITS-X), 40 μg/mL L-proline (Sigma-Aldrich), 200 μM L-ascorbic acid-2-phosphate (Sigma-Aldrich), 100 nM dexamethasone (Sigma-Aldrich), and 10 ng/mL TGF-β1 (PeproTech). Different concentrations of LDN 193189 (Sigma-Aldrich) were used to treat the cells: 0.1, 1, 10, 100, and 1,000 nM. Control microtissues were cultured in chondrogenic medium with vehicle control (0.1% DMSO) but without inhibitor. Chondrogenic cultures were incubated for 14 days at 2% O_2, 5% CO_2, and 37°C. Medium was exchanged every 2 days. To monitor the growth of chondrogenic microtissues, microscope images were captured at days 2, 8, and 14 of culture.

BMSC osteogenic induction cultures

BMSCs were seeded at 6×10^4 cells/cm² in 12-well plates for RNA collection (Nunc) and in 24-well plates (Nunc) for mineralization and adipogenic assays. Osteogenic induction medium contained HG-DMEM supplemented with 10% FBS, 1% PenStrep, 10 mM β-glycerol phosphate (BGP, Sigma-Aldrich), 100 nM dexamethasone, and 50 μM L-ascorbic acid-2-phosphate. Where indicated, 100 ng/mL BMP-2 (Medtronic) was added to the medium. Where indicated, LDN 193189 was added to medium at a concentration of 0.1, 1, 10, 100, or 1,000 nM. Control medium contained osteogenic induction medium components and 0.1% DMSO without BMP-2 or LDN 193189. Cultures were maintained for 9 days to prevent complete delamination, and the medium was exchanged every 3 days. The concentration of BMP-2 added to the BMSC osteogenic cultures was determined by doing a titration experiment wherein increasing concentrations of BMP-2 were added to BMSC cultures for 14 days.

BMSC adipogenic induction cultures

Adipogenic induction medium contained HG-DMEM, 10% FBS, 1% PenStrep, 1 μg/mL insulin (Gibco), 100 nM dexamethasone, 200 μM indomethacin (Sigma-Aldrich), and 500 μM 3-isobutyl-1-methylxanthine (IBMX, Sigma-Aldrich). Where indicated, LDN 193189 was added to medium at a concentration of 0.1, 1, 10, 100, or 1,000 nM. Control medium contained only adipogenic induction medium components and 0.1% DMSO without LDN 193189. Cultures were maintained for 21 days, and the medium

was exchanged every 3 days. BMSCs were seeded at 6×10^4 cells/cm² in 12-well plates for RNA collection (Nunc) and in -well plates (Nunc) for adipogenic assays.

GAG and DNA quantification in chondrogenic induction cultures

Microtissues were harvested following 14 days of induction culture. GAG and DNA were quantified as described previously (Futrega et al., 2015). Briefly, microtissues were digested in 125 μg/mL papain (Sigma-Aldrich) in 100 mM PBE buffer at pH 6.5 overnight at 60°C. DNA in the digest was quantified using a Quant-iT PicoGreen dsDNA Assay Kit (Thermo Fisher Scientific) as recommended by the manufacturer, and fluorescence was read in a microplate reader (FLUOstar Omega) at 485 nm excitation and 520 nm emission. Quantification of GAG in the papain-digested samples was performed using the dimethylmethylene blue (DMMB; Sigma-Aldrich) assay. The plate was read using a microplate reader at 540 nm (Multiskan Go; Thermo Fisher Scientific), and GAG was estimated using a standard curve of serial dilutions of chondroitin sulfate derived from shark cartilage (Sigma-Aldrich).

Microtissue histology

At harvest, microtissues were washed with PBS and fixed overnight in 4% paraformaldehyde (PFA, Sigma). Fixed samples were embedded in Tissue-Tek optimal cutting temperature compound (OCT, Sakura Finetek) and stored at −20°C. Cryosectioning was performed using a Leica Cryostat CM 1950, and 7-μm sections were collected on poly-lysine coated slides (Thermo Fisher). Microtissue sections were gently washed with PBS to remove OCT, and slides were fixed in 4% PFA for 30 min and then stained with Alcian blue (Sigma) stain (Schmitz et al., 2010). Slides were coverslipped using Eukitt mounting medium (Sigma-Aldrich), and sections were imaged with an Olympus BX61 microscope.

Immunohistochemistry

Tissue sections (microtissues and native cartilage for control) were gently washed with PBS to remove OCT, and slides were fixed in 4% PFA for 30 min. The collection of cartilage tissue was approved by the Holy Spirit North Side Hospital Human Ethics Committee and the Queensland University of Technology Human Research Ethics Committee (Ethics No. 1400001024). All tissue collection and ethics approvals were as per the Australian National Health and Medical Research Council guidelines. Tissue sections were then treated with 2 mg/mL hyaluronidase (Sigma-Aldrich), permeabilized with 0.1% Triton X-100 (Sigma-Aldrich), and blocked with 10% normal goat serum (Thermo Fisher). Sections were stained with the following primary antibodies (Abcam): anti-collagen type II (ab34712) and anti-collagen type X (ab58632). Primary antibodies were suspended in 1% BSA (Sigma-Aldrich) and incubated on tissue sections overnight at 4°C. The secondary antibody (goat anti-rabbit IgG-HRP; ab6721, Abcam) were applied the following day at room temperature for 1 h, and the DAB chromogen kit (Abcam) was used to stain the sections per the manufacturer's instructions. Tissue sections were counterstained with hematoxylin (Sigma-Aldrich).

Slides were coverslipped using Eukitt mounting medium, and sections were imaged with an Olympus BX61 microscope.

Relative cell viability of osteogenic and adipogenic cultures

Following 9 days of osteogenic induction and 21 days of adipogenic induction culture, the relative cell viability was measured using the alamarBlue assay (Thermo Fisher) per the manufacturer's recommendations. Cultures were incubated for 3 h at 37°C, and then fluorescence was read using a fluorescence spectrophotometer (FLUOstar Omega), using spectral excitation/emission of 544 and 590 nm.

Detection of mineralization in osteogenic cultures

Following the specified days of culture, monolayers were fixed with 4% PFA for 30 min and then stained with alizarin red S (Sigma-Aldrich) for 10 min on a rocker. Excess stain was repeatedly washed out with distilled water. Bright-field images were captured using an Olympus BX61 microscope. Calcium deposits were quantified using the OCPC assay (Futrega et al., 2018).

Lipid staining and quantification

Osteogenic and adipogenic cultures were washed with PBS, fixed with 4% PFA for 30 min, and stained with oil red O stain (Sigma-Aldrich) for 15 min. Excess stain was washed out with distilled water. Bright-field images were captured using an Olympus BX61 microscope. Estimation of area with lipid vacuoles in culture wells was done by image analysis (ImageJ version 1.53a) using images (n = 30) from different regions of each replicate well per sample, per condition.

Gene expression quantification using qRT-PCR

Total RNA was isolated using the RNeasy Mini Kit (Qiagen), following the manufacturer's instructions. Chondrogenic microtissues were additionally crushed in microcentrifuge tubes using micropestles (Sigma-Aldrich). Samples were treated on-column with DNase-I (Qiagen) in accordance with the manufacturer's protocol. RNA concentration and purity were measured using a Nano-Drop 1000 spectrophotometer (Thermo Fisher Scientific).

Extracted RNA was reverse transcribed using a SensiFAST cDNA Synthesis Kit (Bioline) to produce cDNA. Synthesized cDNA was combined with forward and reverse primers (200 nM), and SYBR Green PCR Master Mix (Applied Biosystems) and analyzed on a Viia7 Real-Time PCR System (Applied Biosystems). Primer sequences are detailed in Table S1. *GAPDH* was used as a housekeeping gene for chondrogenic, osteogenic, and adipogenic samples. The run parameters were as follows: a single initial cycle of 50°C for 2 min and 95°C for 10 min, followed by 40 cycles of 95°C for 15 s and 60°C for 1 min. Target gene expression relative to housekeeping gene expression was calculated using the formula, $2\hat{\ }(C_T[\text{gene of interest}] - C_T[GAPDH])$.

Statistical analysis

Quantitative values were generated from four unique BMSC donors, with four biological replicate cultures per BMSC donor for chondrogenic differentiation and three biological replicate cultures per BMSC donor for osteogenic and adipogenic differentiation assays. All compared data were assessed for normal distribution using the Shapiro-Wilks test (α = 0.05). For datasets that deviated from normal distribution, the statistical analysis was completed using the Kruskal-Wallis test. For microtissue size comparison, which included data from three time points, two-way ANOVA was performed with Dunnett's multiple comparison tests. For qPCR analysis, individual donor analysis was completed using one-way ANOVA with Dunnett's multiple comparison test.

REFERENCES

Amin, H.D., Brady, M.A., St-Pierre, J.-P., Stevens, M.M., Overby, D.R., and Ethier, C.R. (2014). Stimulation of chondrogenic differentiation of adult human bone marrow-derived stromal cells by a moderate-strength static magnetic field. Tissue Eng. *20*, 1612–1620.

Babur, B.K., Futrega, K., Lott, W.B., Klein, T.J., Cooper-White, J., and Doran, M.R. (2015). High-throughput bone and cartilage micropellet manufacture, followed by assembly of micropellets into biphasic osteochondral tissue. Cell Tissue Res. *361*, 755–768.

Boergermann, J.H., Kopf, J., Yu, P.B., and Knaus, P. (2010). Dorsomorphin and LDN-193189 inhibit BMP-mediated Smad, p38 and Akt signalling in C2C12 cells. Int. J. Biochem. Cell Biol. *42*, 1802–1807.

Chawla, S., Berkelaar, M.H.M., Dasen, B., Halleux, C., Guth-Gundel, S., Kramer, I., Ghosh, S., Martin, I., Barbero, A., and Occhetta, P. (2020). Blockage of bone morphogenetic protein signalling counteracts hypertrophy in a human osteoarthritic micro-cartilage model. J. Cell Sci. *133*, jcs249094.

Cleary, M.A., Narcisi, R., Albiero, A., Jenner, F., de Kroon, L.M.G., Koevoet, W.J.L.M., Brama, P.A.J., and van Osch, G.J.V.M. (2017). Dynamic regulation of TWIST1 expression during chondrogenic differentiation of human bone marrow-derived mesenchymal stem cells. Stem Cell. Dev. *26*, 751–761.

Dexheimer, V., Frank, S., and Richter, W. (2012). Proliferation as a requirement for in vitro chondrogenesis of human mesenchymal stem cells. Stem Cell. Dev. *21*, 2160–2169.

Dexheimer, V., Gabler, J., Bomans, K., Sims, T., Omlor, G., and Richter, W. (2016). Differential expression of TGF-β superfamily members and role of Smad1/5/9-signalling in chondral versus endochondral chondrocyte differentiation. Sci. Rep. *6*, 36655.

Dreher, S.I., Fischer, J., Walker, T., Diederichs, S., and Richter, W. (2020). Significance of MEF2C and RUNX3 regulation for endochondral differentiation of human mesenchymal progenitor cells. Front. Cell Dev. Biol. *8*, 81.

Freyria, A.M., and Mallein-Gerin, F. (2012). Chondrocytes or adult stem cells for cartilage repair: the indisputable role of growth factors. Injury *43*, 259–265.

Futrega, K., Palmer, J.S., Kinney, M., Lott, W.B., Ungrin, M.D., Zandstra, P.W., and Doran, M.R. (2015). The microwell-mesh: a novel device and protocol for the high throughput manufacturing of cartilage microtissues. Biomaterials *62*, 1–12.

Futrega, K., Mosaad, E., Chambers, K., Lott, W.B., Clements, J., and Doran, M.R. (2018). Bone marrow-derived stem/stromal cells (BMSC) 3D microtissues cultured in BMP-2 supplemented osteogenic induction medium are prone to adipogenesis. Cell Tissue Res. *374*, 541–553.

Futrega, K., Robey, P.G., Klein, T.J., Crawford, R.W., and Doran, M.R. (2021). A single day of TGF-β1 exposure activates chondrogenic and hypertrophic differentiation pathways in bone marrow-derived stromal cells. Commun. Biol. *4*, 29.

Goldberg, A., Mitchell, K., Soans, J., Kim, L., and Zaidi, R. (2017). The use of mesenchymal stem cells for cartilage repair and regeneration: a systematic review. J. Orthop. Surg. Res. *12*, 39.

Grayson, W.L., Zhao, F., Izadpanah, R., Bunnell, B., and Ma, T. (2006). Effects of hypoxia on human mesenchymal stem cell expansion and plasticity in 3D constructs. J. Cell. Physiol. *207*, 331–339.

Grayson, W.L., Zhao, F., Bunnell, B., and Ma, T. (2007). Hypoxia enhances proliferation and tissue formation of human mesenchymal stem cells. Biochem. Biophys. Res. Commun. *358*, 948–953.

Handorf, A.M., and Li, W.J. (2014). Induction of mesenchymal stem cell chondrogenesis through sequential administration of growth factors within specific temporal windows. J. Cell. Physiol. *229*, 162–171.

Hellingman, C.A., Davidson, E.N.B., Koevoet, W., Vitters, E.L., van den Berg, W.B., van Osch, G.J.V.M., and van der Kraan, P.M. (2010). Smad signaling determines chondrogenic differentiation of bone-marrow-derived mesenchymal stem cells: inhibition of Smad1/5/8P prevents terminal differentiation and calcification. Tissue Eng. *17*, 1157–1167.

Jakobsen, R.B., Ostrup, E., Zhang, X., Mikkelsen, T.S., and Brinchmann, J.E. (2014). Analysis of the effects of five factors relevant to in vitro chondrogenesis of human mesenchymal stem cells using factorial design and high throughput mRNA-profiling. PLoS One *9*, e96615.

Katagiri, T., and Watabe, T. (2016). Bone morphogenetic proteins. Cold Spring Harbor Perspect. Biol. *8*, a021899.

Kim, H.-J., and Im, G.-I. (2009). The effects of ERK1/2 inhibitor on the chondrogenesis of bone marrow– and adipose tissue–derived multipotent mesenchymal stromal cells. Tissue Eng. *16*, 851–860.

Kim, Y.-J., Kim, H.-J., and Im, G.-I. (2008). PTHrP promotes chondrogenesis and suppresses hypertrophy from both bone marrow-derived and adipose tissue-derived MSCs. Biochem. Biophys. Res. Commun. *373*, 104–108.

Kovermann, N.J., Basoli, V., Della Bella, E., Alini, M., Lischer, C., Schmal, H., Kubosch, E.J., and Stoddart, M.J. (2019). BMP2 and TGF-β cooperate differently during synovial-derived stem-cell chondrogenesis in a dexamethasone-dependent manner. Cells *8*, 636.

Lee, J.-M., and Im, G.-I. (2012). PTHrP isoforms have differing effect on chondrogenic differentiation and hypertrophy of mesenchymal stem cells. Biochem. Biophys. Res. Commun. *421*, 819–824.

Marcu, K.B., de Kroon, L.M.G., Narcisi, R., Blaney Davidson, E.N., Cleary, M.A., van Beuningen, H.M., Koevoet, W.J.L.M., van Osch, G.J.V.M., and van der Kraan, P.M. (2015). Activin receptor-like kinase receptors ALK5 and ALK1 are both required for TGFβ-induced chondrogenic differentiation of human bone marrow-derived mesenchymal stem cells. PLoS One *10*, e0146124.

Markway, B.D., Tan, G.K., Brooke, G., Hudson, J.E., Cooper-White, J.J., and Doran, M.R. (2010). Enhanced chondrogenic differentiation of human bone marrow-derived mesenchymal stem cells in low oxygen environment micropellet cultures. Cell Transplant. *19*, 29–42.

Martin-Rendon, E., Hale, S.J.M., Ryan, D., Baban, D., Forde, S.P., Roubelakis, M., Sweeney, D., Moukayed, M., Harris, A.L., Davies, K., et al. (2007). Transcriptional profiling of human cord blood CD133+ and cultured bone marrow mesenchymal stem cells in response to hypoxia. Stem Cells *25*, 1003–1012.

Moussavi-Harami, F., Duwayri, Y., Martin, J.A., Moussavi-Harami, F., and Buckwalter, J.A. (2004). Oxygen effects on senescence in chondrocytes and mesenchymal stem cells: consequences for tissue engineering. Iowa Orthop. J. *24*, 15–20.

Narcisi, R., Cleary, M.A., Brama, P.A., Hoogduijn, M.J., Tuysuz, N., ten Berge, D., and van Osch, G.J. (2015). Long-term expansion, enhanced chondrogenic potential, and suppression

of endochondral ossification of adult human MSCs via WNT signaling modulation. Stem Cell Rep. *4*, 459–472.

Negoro, T., Takagaki, Y., Okura, H., and Matsuyama, A. (2018). Trends in clinical trials for articular cartilage repair by cell therapy. NPJ Regen. Med. *3*, 17.

Occhetta, P., Pigeot, S., Rasponi, M., Dasen, B., Mehrkens, A., Ullrich, T., Kramer, I., Guth-Gundel, S., Barbero, A., and Martin, I. (2018). Developmentally inspired programming of adult human mesenchymal stromal cells toward stable chondrogenesis. Proc. Natl. Acad. Sci. U S A *115*, 4625–4630.

Puetzer, J.L., Petitte, J.N., and Loboa, E.G. (2010). Comparative review of growth factors for induction of three-dimensional in vitro chondrogenesis in human mesenchymal stem cells isolated from bone marrow and adipose tissue. Tissue Eng. B Rev. *16*, 435–444.

Rosen, E.D., Hsu, C.H., Wang, X., Sakai, S., Freeman, M.W., Gonzalez, F.J., and Spiegelman, B.M. (2002). C/EBPalpha induces adipogenesis through PPARgamma: a unified pathway. Genes Dev. *16*, 22–26.

Schmitz, N., Laverty, S., Kraus, V.B., and Aigner, T. (2010). Basic methods in histopathology of joint tissues. Osteoarthritis Cartilage *18*, S113–S116.

Somoza, R.A., Welter, J.F., Correa, D., and Caplan, A.I. (2014). Chondrogenic differentiation of mesenchymal stem cells: challenges and unfulfilled expectations. Tissue Eng. B Rev. *20*, 596–608.

Sottile, V., and Seuwen, K. (2000). Bone morphogenetic protein-2 stimulates adipogenic differentiation of mesenchymal precursor cells in synergy with BRL 49653 (rosiglitazone). FEBS Lett. *475*, 201–204.

Takada, I., Yogiashi, Y., and Kato, S. (2012). Signaling crosstalk between PPARγ and BMP2 in mesenchymal stem cells. PPAR Res. *2012*, 607141.

Wu, C.-L., Dicks, A., Steward, N., Tang, R., Katz, D.B., Choi, Y.-R., and Guilak, F. (2021). Single cell transcriptomic analysis of human pluripotent stem cell chondrogenesis. Nat. Commun. *12*, 362.

Yang, Z., Zou, Y., Guo, X.M., Tan, H.S., Denslin, V., Yeow, C.H., Ren, X.F., Liu, T.M., Hui, J.H., and Lee, E.H. (2012). Temporal activation of beta-catenin signaling in the chondrogenic process of mesenchymal stem cells affects the phenotype of the cartilage generated. Stem Cell. Dev. *21*, 1966–1976.

Yu, P.B., Deng, D.Y., Lai, C.S., Hong, C.C., Cuny, G.D., Bouxsein, M.L., Hong, D.W., McManus, P.M., Katagiri, T., Sachidanandan, C., et al. (2008). BMP type I receptor inhibition reduces heterotopic [corrected] ossification. Nat. Med. *14*, 1363–1369.

Zscharnack, M., Poesel, C., Galle, J., and Bader, A. (2009). Low oxygen expansion improves subsequent chondrogenesis of ovine bone-marrow-derived mesenchymal stem cells in collagen type I hydrogel. Cells Tissues Organs *190*, 81–93.